Hierarchical Morse Complexes for Piecewise Linear 2-Manifolds *

Herbert Edelsbrunner†, John Harer‡, and Afra Zomorodian§

[Manuscript - Do Not Distribute - June 14, 2001]

Abstract

We present algorithms for constructing a hierarchy of increasingly coarse Morse complexes that decompose a piecewise linear 2-manifold. While Morse complexes are defined only in the smooth category, we extend the construction to the piecewise linear category by ensuring structural integrity and simulating differentiability. We then simplify Morse complexes by cancelling pairs of critical points in order of increasing persistence.

Keywords. Computational topology, PL manifolds, Morse theory, topological persistence, hierarchy, algorithms, implementation, terrains.

1 Introduction

In this paper, we define the Morse complex decomposing a piecewise linear 2-manifold and present algorithms for constructing and simplifying this complex.

Motivation. Physical simulation problems often start with a space and measurements over this space. If the measurements are scalar values, we talk about a height function of that space. We use this name throughout the paper, although the functions can be arbitrary and do not necessarily measure height. Two-dimensional examples of height functions include intensity values of an image, and the elevation of a terrain as parametrized by longitude and latitude. Three-dimensional examples include the temperature within a room, volume intensities produced by magnetic resonance imaging, and the electron density over a crystallized molecule. In all these examples, we seek to derive structures that enhance our understanding of the measurements.

Consider a geographic landscape modeled as a height function $h : D \to \mathbb{R}$ over a two-dimensional domain D. We can visualize h by discrete set of iso-lines $h^{-1}(c)$ of constant height values. The topological structure of iso-lines is partially captured by the contour tree [3, 4, 14]. If h is differentiable, we may define the gradient field consisting of vectors in the direction of the steepest ascent. Researchers in visualization have studied this vector field for some time [1, 5, 13]. The Morse complex captures the characteristics of this vector field by decomposing the manifold into cells of uniform flow. As such, the Morse complex represents a full analysis of the behavior of the vector field.

Often, however, the smooth domain D is sampled. No matter how dense the sampling, we encounter two critical issues: our theoretical notions, based on smooth structures, are no longer valid, and we have to distinguish between noise and features in the sampled data. Our goal in this work is resolve both issues in the piecewise linear (PL) domain.

Methods and Results. To extend smooth notions to PL manifolds, we use differential structures to guide our computations. We call this method the *simulation of differentiability* or *SoD* paradigm. Using SoD, we first guarantee the computed complexes have the same structural form as those in the smooth case. We then achieve numerical accuracy by means of transformations that maintain this structural integrity. The separation of combinatorial and numerical aspects of computation is similar to many algorithms in computational geometry. It is also the hallmark of the SoD paradigm. Our results are:

(i) an algorithm for constructing a complex whose combinatorial form matches that of the Morse complex,

(ii) an algorithm for deriving the Morse complex from the complex in (i) via local transformations,

(iii) an algorithm for constructing a hierarchy of Morse complexes, again via local transformations,

(iv) and the application of the algorithms to geographic terrain data.

*Research by the first and third authors are partially supported by ARO under grant DAAG55-98-1-0177. Research by the first author is also partially supported by NSF under grants CCR-97-12088, EIA-9972879, and CCR-00-86013.

†Department of Computer Science, Duke University, Durham, and Raindrop Geomagic, Research Triangle Park, NC.

‡Department of Mathematics, Duke University, Durham, NC.

§Department of Computer Science, University of Illinois, Urbana, IL.

Because of the theoretical nature of our endeavor, we devote most of our effort in this paper to (i) through (iii). While we include only a short section on (iv), we view this paper as the foundation for creating robust software for the scientific and engineering fields.

Outline. The rest of the paper is organized as follows. In Section 2, we introduce the theoretical background from Morse theory on smooth 2-manifolds. In Section 3, we extend these notions to PL domains, and discuss difficulties resulting from the absence of smoothness. Having computed a structurally correct complex in Section 4, we compute the Morse complex via transformations in Section 5. We introduce topological persistence in Section 6, and use it to create a hierarchy of complexes in Section 7. We give some experimental results for geographic landscapes in Section 8, concluding the paper in Section 9.

2 Smooth 2-Manifolds

In this section, we introduce concepts from Morse theory we need as the theoretical background for our work. We refer to Milnor [10] and Wallace [15] for further background.

Morse functions. Let $\mathbb{M}$ be a smooth, compact 2-manifold without boundary and let $h : \mathbb{M} \to \mathbb{R}$ be a smooth map. The differential of h at the point a is a linear map $dh_a : \mathrm{T}\mathbb{M}_a \to \mathrm{T}\mathbb{R}_{h(a)}$ mapping the tangent space to $\mathbb{M}$ at a to that of $\mathbb{R}$ at $h(a)$. (The tangent space to $\mathbb{R}$ at a point is simply $\mathbb{R}$ again, with the origin shifted to that point.) A point a is called *critical* if the map dh_a is the zero map. Otherwise, it is a *regular* point. At a critical point a we compute in local coordinates the *Hessian* of h,

$$H(a) \quad = \quad \begin{bmatrix} \frac{\partial^2 h}{\partial x^2}(a) & \frac{\partial^2 h}{\partial y \partial x}(a) \\ \frac{\partial^2 h}{\partial x \partial y}(a) & \frac{\partial^2 h}{\partial y^2}(a) \end{bmatrix}.$$

The Hessian is a symmetric bilinear form on the tangent space $\mathrm{T}\mathbb{M}_a$ of $\mathbb{M}$ at a. The matrix above expresses this functional in terms of the basis $(\frac{\partial}{\partial x}(a), \frac{\partial}{\partial y}(a))$ for $\mathrm{T}\mathbb{M}_a$. A critical point a is called *non-degenerate* if the Hessian is non-singular at a, i.e. $\det H(a) \neq 0$, a property that is independent of the coordinate system. The Morse Lemma [10] states that near a non-degenerate critical point it is possible to choose local coordinates so that h takes the form

$$h(x, y) \quad = \quad \pm x^2 \pm y^2.$$

The number of minuses is called the *index* $i(a)$ of h at the critical point a; it equals the number of negative eigenvalues of $H(a)$ or equivalently, the index of the functional $H(a)$. Note that the existence of these local coordinates implies that non-degenerate critical points are isolated.

In two dimensions, there are three types of non-degenerate critical points: *minima* have index 0, *saddles* have index 1, and *maxima* have index 2. The function h is called a *Morse function* if all its critical points are non-degenerate (sometimes one also requires that the critical *values* of h, that is, the values that h takes at its critical points, are distinct. We will not need this requirement here.) Any twice differentiable function h can be unfolded to a Morse function.

Stable and unstable manifolds. In order to measure angles and lengths for tangent vectors, we choose a Riemannian metric $\langle , \rangle$ on $\mathbb{M}$, i.e. an inner product in each tangent space $\mathrm{T}\mathbb{M}_a$ that varies smoothly over $\mathbb{M}$. Since each vector in $\mathrm{T}\mathbb{M}_a$ is the tangent to a curve γ in $\mathbb{M}$ through a, the *gradient* of h, ∇h, can be defined by the formula

$$\langle \frac{d\gamma}{dt}, \nabla h \rangle \quad = \quad \frac{d(h \circ \gamma)}{dt},$$

for every γ. It is always possible to choose coordinates (x, y) so that the tangent vectors $\frac{\partial}{\partial x}(a)$, $\frac{\partial}{\partial y}(a)$ are orthonormal with respect to $\langle , \rangle$. For such coordinates, the gradient is given by the familiar formula $\nabla h = (\frac{\partial h}{\partial x}(a), \frac{\partial h}{\partial y}(a))$.

An *integral line* $p : \mathbb{R} \to \mathbb{M}$ is a maximal path whose tangent vectors agree with the gradient, that is, $\frac{\partial}{\partial s} p(s) = \nabla h(p(s))$ for all $s \in \mathbb{R}$. Each integral line is open at both ends. We call $\operatorname{org} p = \lim_{s \to -\infty} p(s)$ the *origin* and $\operatorname{dest} p = \lim_{s \to +\infty} p(s)$ the *destination* of the path p. These limits both exist because $\mathbb{M}$ is compact. Integral lines have the following three properties.

(P1) Two integral lines are either disjoint or the same.

(P2) The integral lines cover all of $\mathbb{M}$.

(P3) The limits $\operatorname{org} p$ and $\operatorname{dest} p$ are critical points of h.

We use these properties to decompose $\mathbb{M}$ into regions of uniform flow. The *stable manifold* $S(a)$ and the *unstable manifold* $U(a)$ of a critical point a are defined as

$$\begin{aligned} S(a) &= \{a\} \cup \{y \in \mathbb{M} \mid y \in \operatorname{im} p, \operatorname{dest} p = a\}, \\ U(a) &= \{a\} \cup \{y \in \mathbb{M} \mid y \in \operatorname{im} p, \operatorname{org} p = a\}, \end{aligned}$$

where $\operatorname{im} p$ is the image of the path p. Note that the unstable manifolds of h are the stable manifolds of $-h$ as $\nabla(-h) = -\nabla(h)$. Therefore, the two types of manifolds have the same structural properties. An *open cell* of dimension i is a space homeomorphic to $\mathbb{R}^i$. The stable manifold $S(a)$ of a critical point a with index $i = i(a)$ is an open cell of dimension $\dim S(a) = i$. The closure of a stable manifold, however, is not necessarily homeomorphic to a closed ball, as seen in Figure 1. By properties (P1), (P2), and (P3), the stable manifolds are pairwise disjoint and decompose $\mathbb{M}$ into open cells. The cells form a complex, as the boundary of every cell $S(a)$ is the union of lower-dimensional cells, its *faces*. The unstable manifolds similarly decompose $\mathbb{M}$ into a complex dual to the complex of stable manifolds: for $a, b \in \mathbb{M}$, $\dim S(a) = 2 - \dim U(a)$, and $S(a)$ is a face of $S(b)$ iff $U(b)$ is a face of $U(a)$.

Morse complex. A Morse function h is a *Morse-Smale function* if the stable and unstable manifolds intersect only transversally. In two dimensions, this means that stable and unstable 1-manifolds cross when they intersect. Their crossing point is necessarily a saddle, since crossing at a regular point would contradict property (P1). We intersect the stable and unstable manifolds to obtain the *Morse cells* as the connected components of the sets $U(a) \cap S(b)$, for all critical points $a, b \in \mathbb{M}$. Note that $U(a) \cap S(a) = \{a\}$, and if $a \neq b$, then $U(a) \cap S(b)$ is the set of regular points $y \in \mathbb{M}$ that lie on integral lines p with $\operatorname{org} p = a$ and $\operatorname{dest} p = b$. It is possible that the intersection consists of more than one component, as seen in Figure 1. We refer to the cells of dimension 0, 1, and 2 as *vertices*, *arcs*, and *regions*, respectively. Each vertex is a critical point, each arc is half of a stable or unstable 1-manifold, and each region is a component of the intersection of a stable and an unstable 2-manifold. We prove that the regions have a special shape.

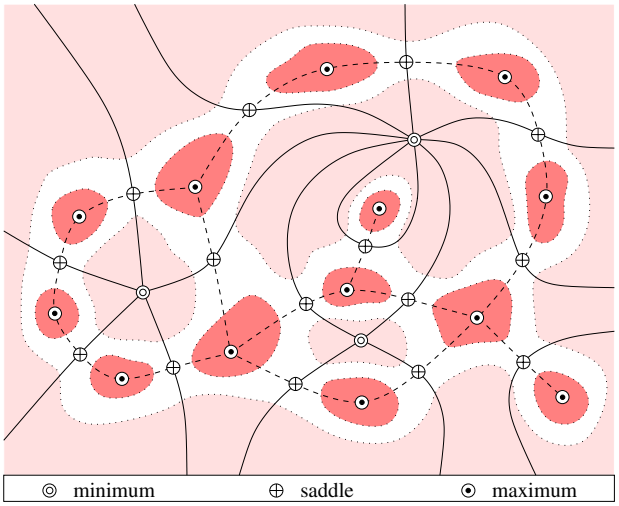

Figure 1: A Morse complex with solid stable 1-manifolds and dashed unstable 1-manifolds. In drawing the dotted iso-lines we assume that all saddles have height between all minima and all maxima.

QUADRANGLE LEMMA. Each region of the Morse complex is a quadrangle with vertices of index 0, 1, 2, 1, in this order around the region. The boundary is possibly glued to itself along vertices and arcs.

PROOF. The vertices on the boundary of any region alternate between saddles and other critical points, which, in turn, alternate between maxima and minima. The shortest possible cyclic sequence of vertices around a boundary is therefore 0, 1, 2, 1, a quadrangle. We prove below that longer sequences force a critical point in the interior of the region, a contradiction.

We take a region whose boundary cycle has length $4k$ for $k \geq 2$ and glue two copies of the region together along their boundary to form a sphere. We glue each critical point to its copy, so saddles become regular points, maxima and minima remain as before. The Euler characteristic of the sphere is 2, and so is the alternating sum of critical points, $\sum_a (-1)^{i(a)}$. However, the number of minima and maxima together is $2k > 2$, which implies that there is at least one saddle inside the region. ◻

Quasi Morse complexes. Intuitively, we define a quasi Morse complex to be a complex with the structural form of a Morse complex. It is combinatorially a quadrangulation with vertices at the critical points of h and with edges that strictly ascend and descend as measured by h, but it differs in that its edges may not necessarily be the edges of maximal ascent and descent. A subset of the vertices in a complex Q is *independent* if no two are connected by an arc. The complex Q is *splitable* if we can partition the vertices into three sets U, V, W and the arcs into two sets A, B so that

(i) $U \cup W$ and V are both independent,

(ii) arcs in A have endpoints in $U \cup V$ and arcs in B have endpoints in $V \cup W$, and

(iii) each vertex $v \in V$ belongs to four arcs, which in a cyclic order around v alternate between A and B.

We may then *split* Q into two complexes defined by U, A and W, B. Note that the Morse complex is splitable: (i) U, V, and W are the maxima, saddles, and minima, (ii) A connects maxima to saddles and B connects minima to saddles, and (iii) saddles have degree four and alternate as required. The Morse complex then splits into the complex of stable and the complex of unstable manifolds.

A *splitable quadrangulation* is a splitable complex whose regions are quadrangles. We define a *quasi Morse complex* of a 2-manifold $\mathbb{M}$ and a height function h as a splitable quadrangulation whose vertices are the critical points of h and whose arcs are monotone in height.

3 PL 2-Manifolds

The gradient of a PL height function is not continuous and does not generate the pairwise disjoint integral lines that are needed to define stable and unstable manifolds. In this section, we deal with the resulting difficulties by simulating differentiability using infinitesimal bump functions. Such a simulation unfolds degenerate critical points and turns stable and unstable manifolds into open cells, as needed.

Triangulation and stars. Let K be a triangulation of a compact 2-manifold without boundary $\mathbb{M}$, and let $h : \mathbb{M} \to \mathbb{R}$ be a PL height function that is linear on every triangle. The height function is thus defined by its values at the vertices of K. It will be convenient to assume $h(u) \neq h(v)$ for all vertices $u \neq v$ in K. We simulate simplicity to justify this assumption computationally [8].

In a triangulation, the natural concept of a neighborhood of a vertex u is the *star*, $\operatorname{St} u$, that consists of u together with the edges and triangles that share u as a vertex. Formally, $\operatorname{St} u = \{\sigma \in K \mid u \leq \sigma\}$, where $u \leq \sigma$ is short for u being a face of σ. Since all vertices have different heights, each edge and triangle has a unique lowest and a unique highest vertex. Following Banchoff,[2] we use this to define the *lower* and *upper stars* of u,

$$\begin{aligned} \underline{\operatorname{St}} u &= \{\sigma \in \operatorname{St} u \mid h(v) \leq h(u),\ v \leq \sigma\}, \\ \overline{\operatorname{St}} u &= \{\sigma \in \operatorname{St} u \mid h(v) \geq h(u),\ v \leq \sigma\}, \end{aligned}$$

These subsets of the star contain the simplices that have u as their highest or their lowest vertex. We may partition K into a collection of either subsets, $K = \dot{\bigcup}_u \underline{\operatorname{St}} u = \dot{\bigcup}_u \overline{\operatorname{St}} u$.

We may also use the lower and upper stars to classify a vertex as regular or critical. We define a *wedge* as a contiguous section of $\operatorname{St} u$ that begins and ends with an edge. As shown in Figure 2, the lower star either contains the entire star or some number $k+1$ of wedges, and the same is true for the upper star. If $\underline{\operatorname{St}} u = \operatorname{St} u$, then $k = -1$ and u is a

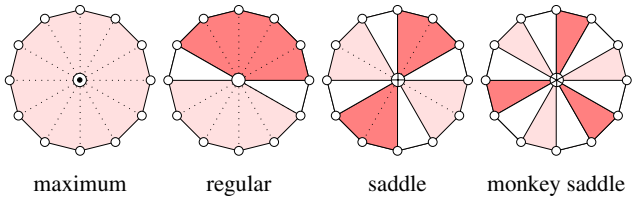

Figure 2: The light shaded lower wedges are connected by white triangles to the dark shaded upper wedges.

maximum. Symmetrically, if $\overline{\operatorname{St}} u = \operatorname{St} u$, then $k = -1$ and u is a minimum. Otherwise, u is regular if $k = 0$, a (simple) saddle if $k = 1$, and a *k-fold* or *multiple saddle* if $k \geq 2$. A 2-fold saddle is often called a *monkey saddle*.

Multiple saddles. We can unfold a k-fold saddle into two saddles of multiplicity $1 \leq i, j < k$ with $i + j = k$ by the following procedure. We split a wedge of $\underline{\operatorname{St}} u$ (through a triangle, if necessary), and similarly split a non-adjacent wedge of $\overline{\operatorname{St}} u$. The new number of (lower and upper) wedges is $2(k+1)+2 = 2(i+1)+2(j+1)$, as required. By repeating the process, we eventually arrive at k simple saddles. The combinatorial process is ambiguous, but it is usually sufficient to pick an arbitrary unfolding from the set of possibilities. For a monkey saddle, there are three ways to minimally unfold, as shown in Figure 3.

Merging and forking. The concept of an integral line for a PL function is not well defined. Instead, we construct monotonic curves that never cross. Such curves can merge together and fork after a while. Moreover, it is possible for two curves to alternate between merging and forking an arbitrary number of times. To resolve this, when two curves merge,

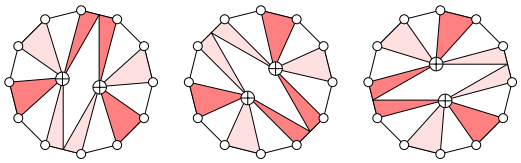

Figure 3: A monkey saddle may be unfolded into two simple saddles in three different ways.

we pretend that they maintain an infinitesimal separation, running side by side without crossing. Figure 4 illustrates

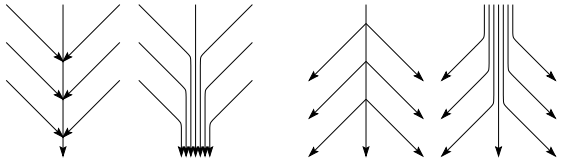

Figure 4: Merging and forking PL curves and their corresponding smooth flow pictures.

the two PL artifacts and the corresponding simulated smooth resolution. The computational simulation of disjoint integral lines is delicate, and uses *junctions* which are the regular points at which ascending and descending paths merge and fork. We give the technical details in Section 4.

Non-transversal intersections. The standard example in Morse theory is the height function over a torus standing on its side. The lowest and highest points of the inner ring are the only saddles, as shown in Figure 5. Both the unstable

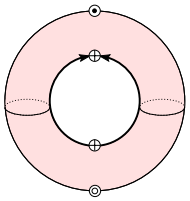

Figure 5: The unstable 1-manifold of the lower saddle approaches the upper saddle.

1-manifold of the lower saddle and the stable 1-manifold of the upper saddle follow the inner ring and overlap in two open half-circles. Generically, such non-transversal intersections do not happen. The characteristic property of a non-transversal intersection is that the unstable 1-manifold of one saddle approaches another saddle, and vice versa. An arbitrarily small perturbation of the height function suffices to make the two 1-manifolds miss the other saddles and approach a maximum and a minimum without meeting each other. The PL counterpart of a non-transversal intersection is an ascending or descending path that ends at a saddle. We

simulate the generic case by extending the path beyond the saddle. Again, we give the details in Section 4.

4 Quasi Morse Complexes

Given a triangulation K of a compact 2-manifold without boundary, and a PL height function h, our goal is to compute the Morse complex for a simulated unfolding of h. In this section, we take a first step, computing a quasi Morse complex of h. We limit ourselves to curves following edges of K. While the resulting complex is numerically inaccurate, we focus on capturing the structure of the Morse complex, and this limitation gives us a fast algorithm. The algorithm proceeds in three stages.

Complex with junctions. In the first stage, we draw paths by following edges in the triangulation. After classifying all vertices and computing the wedges of their lower and upper stars, we determine the steepest edge in each wedge. We start $k+1$ ascending and $k+1$ descending paths from every k-fold saddle. Each path begins in its own wedge and follows a sequence of steepest edges until it hits

(a) a minimum or a maximum,

(b) a previously traced path at a regular point, or

(c) another saddle.

Case (a) corresponds to the generic case for smooth height functions. Case (b) corresponds to a merging or forking, and we either create a new junction by splitting the previously traced path, or we increase the degree of the previously created junction. Case (c) is the PL counterpart of a non-transversal intersection between a stable and an unstable 1-manifold.

We use the quad edge data structure [9] to store the complex defined by the paths. The vertices of the complex are the critical points and junctions, and the arcs are the pairwise edge-disjoint paths connecting these vertices.

Extending paths. In the second stage of our algorithm, we extend paths to remove junctions and reduce the number of arcs per k-fold saddle to $2(k+1)$. Whenever we extend a path, we route it along and infinitesimally close to an already existing path. In doing so, we may create new paths ending at other junctions and saddles. Consequently, we desire to process the vertices in a sequence that prevents cyclic dependencies. But since ascending and descending paths are extended in opposite directions, we need two orderings and we touch every vertex twice. It is convenient to first extend ascending paths in the order of increasing height, and second extend descending paths in the order of decreasing height. We next discuss our routing procedures for junctions and saddles. In the figures that follow, we orient paths in the direction they emanate from a saddle.

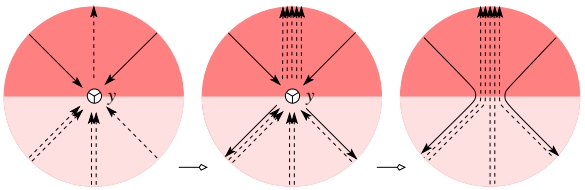

Figure 6: Paths ending at junctions are extended by duplication and concatenation.

Consider the junction y in Figure 6. By definition, y is a regular point with lower and upper stars consisting of one wedge each. The first time we encounter y, the path is traced right through the point. In every additional encounter, the path ends at y. If the first path is ascending, then one ascending path leaves y into the upper star, all other ascending paths approach y from the lower star, and all descending paths approach y from the upper star. Some of the paths may already have duplicates because of other path extensions. We extend paths by first duplicating ascending paths, then duplicating descending paths, and finally concatenating paths in pairs. We can concatenate in order without creating crossings, as shown in Figure 6 to the right.

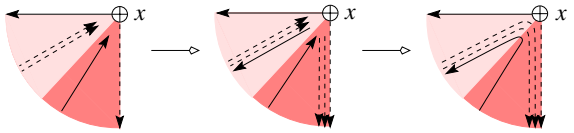

Figure 7: Paths that end at a saddle by Case (c) are extended by duplication and concatenation.

Consider now the saddle x in Figure 7. We look at path extensions only within one of the sectors between two adjacent steepest edges. Within this sector, there may be ascending paths approaching x from within the overlapping wedge of the lower star, and descending paths approaching x from within the overlapping wedge of the upper star, as shown in Figure 7 to the left. We extend paths by first duplicating paths as described before, and then concatenating paths in pairs. Again, we can concatenate without creating crossings.

Unfolding multiple saddles. In the third and last stage of our algorithm, we unfold every k-fold saddle into k simple saddles. As indicated in Figure 3, we can do so simply by duplicating the saddle and paths ending at the saddle. All paths of Case (c) have already been removed in the second stage, so we only have to deal with the $k+1$ ascending and $k+1$ descending paths that originate at the k-fold saddle. In each of the $k-1$ steps, we duplicate the saddle, one ascending path, and a non-adjacent descending path. In the end, we have k saddles and $2(k+1)+2(k-1)=4k$ paths, or four per saddle. Figure 8 illustrates the operation by showing a possible unfolding of a 3-fold saddle.

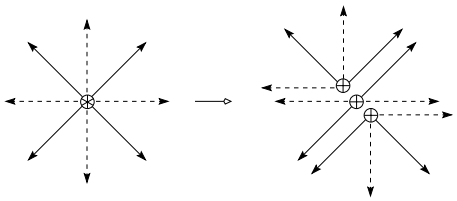

Figure 8: Unfolding a 3-fold saddle into three simple saddles.

5 Local Transformation

We transform a quasi Morse complex to the Morse complex via a sequence of transformations called handle slides. We first describe these transformations, and then present and analyze an algorithm that applies handle slides to the quasi Morse complex.

Handle slide. A handle slide transforms one quasi Morse complex into another. The two quadrangulations differ only in their decompositions of a single octagon. In the first quadrangulation, the octagon consists of a quadrangle $abcd$ together with two adjacent quadrangles $baDC$ and $dcBA$, as shown in Figure 9. We perform a slide by drawing an ascending path from a to B replacing ab, and a descending path from c to D replacing cd. After the slide, the octagon is decomposed into quadrangles $DcBa$ in the middle and $cDCb, aBAd$ on its two sides.

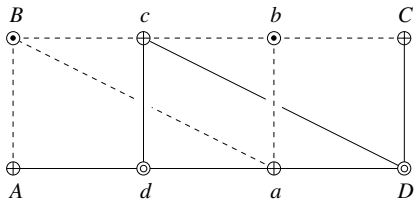

Figure 9: The octagon is the union of a row of three quadrangles. The haloed edges indicate the alternative quadrangulation created by the handle slide.

It is possible to think of the better known edge-flip in a 2-dimensional triangulation as the composition of two octagon slides. To explain this, we superimpose a triangulation with its dual diagram, making sure that only corresponding edges cross, as in Figure 10. The vertices of the triangulation correspond to minima, the vertices of the dual diagram to maxima, and the crossing points to saddles. When we flip an edge in the triangulation, we also reconnect the five edges in the dual diagram that correspond to the five edges of the two triangles sharing the flipped edge. The result of the edge-flip is thus the same as that of two octagon slides, one for the lower left three quadrangles, and the other for the upper right three quadrangles in Figure 10.

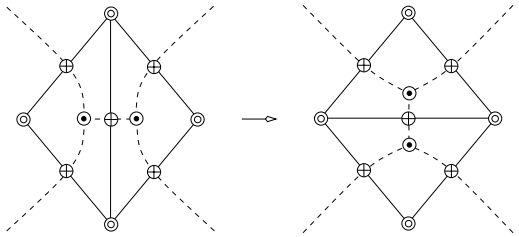

Figure 10: Edge-flip shown in super-imposition of solid triangulation with its dashed dual diagram. The maxima before and after the flip should be at the same location but are moved for clarity of the illustration.

Steepest ascent. We decide whether or not to apply a handle slide to an octagon by rerouting its interior paths. We reroute an ascending path by following the direction of locally steepest ascent, which may go along an edge or pass through a triangle of K. There are three cases as shown in Figure 11. In the interior of a triangle uvw, that steepest direction is unique and orthogonal to the level lines. In the interior of an edge, there may be one or two locally steepest directions, and at a vertex there may be as many locally steepest directions as there are triangles in the star. We may compute the globally steepest direction numerically with small error, but errors accumulate as the path traverses triangles. Alternatively, we can compute the globally steepest direction exactly with constant bit-length arithmetic operations, but the bit-length needed for the points along the path grows as it traverses more triangles. This phenomenon justifies the SoD approach to constructing a Morse complex. In that approach the computed complex has the same combinatorial form as the Morse complex, and it is numerically as accurate as the local rerouting operations used to control handle slides.

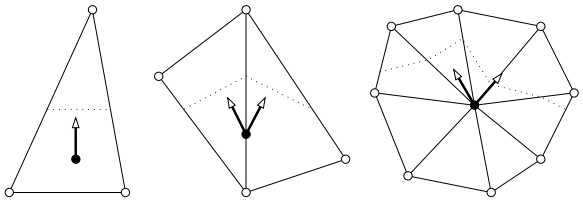

Figure 11: The directions of locally steepest ascent are orthogonal to the dotted level lines.

Algorithm. We now describe how transformations are applied to construct the Morse complex. The algorithm applies handle slides in the order of decreasing height, where the *height* of an octagon is the height of the lower saddle of the middle quadrangle. In Figure 9, this saddle is either a or c, and we assume here that it is a. At the time we consider a, we may assume that the arcs connecting higher critical points are already correct. The iso-line at the height of a de-

composes the manifold into an *upper* and a *lower region*, and we let Γ be the possibly pinched component of the upper region that contains a. There are two cases, as shown in Figure 12. In the first case, the higher critical points in Γ and their connecting arcs bound one annulus, which is pinched at a, while in the second case they bound two annuli, one on each side of a. The ascending path emanating from a is rerouted within these annuli.

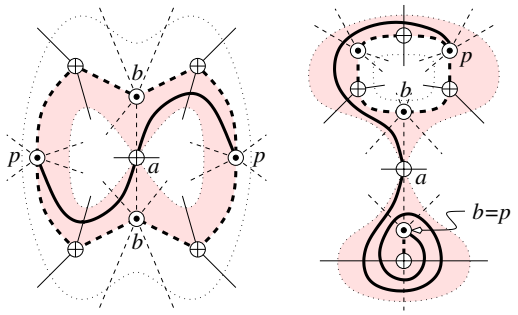

Figure 12: The iso-line is dotted, the annuli are shaded, the arcs bounding the annuli are bold dashed, and the new paths emanating from a are bold solid.

Let ab be the interior path of the octagon with height $h(a)$, and let p be the maximum we hit by rerouting the path. If p is the first maximum after b along the arc boundary of the annulus, we may use a single handle slide to replace ab by ap, as we do for the upper new path in Figure 12 to the left. Note that the slide is possible only because ap crosses no arc ending at b. Any such arc would have to be changed first, which we do by recursive application of the algorithm, as for the lower new path in Figure 12 to the left. It is also possible that p is more than one position removed from b, as for the upper new path in Figure 12 to the right. In this case we perform several slides for a, the first connecting a to the first maximum after b in the direction of p. Each such slide may require recursive slides to clear the way, as before. Finally, it is possible that the new path from a to p winds around the arc boundary of the annulus several times, as does the lower new path in Figure 12 to the right. The algorithm is the same as before.

The winding case shows that the number of slides cannot be bounded from above in terms of the number of critical points. Instead we consider crossings between arcs of the initial quasi Morse and the final Morse complexes, and note that the number of slides is at most some constant times the number of such crossings.

6 Topological Persistence

We may measure the importance of every critical point and construct a hierarchy of complexes by eliminating critical points with measure below a threshold. In this section, we describe a measure called persistence and discuss its computation. Further details may be found in [7].

Filtration and Betti numbers. Assume we assemble the triangulation K of a connected compact 2-manifold without boundary $\mathbb{M}$ by adding simplices in the order of increasing height. Let $u^1, u^2, \ldots, u^n$ be the sequence of vertices such that $h(u^i) < h(u^j)$ for all $1 \leq i < j \leq n$, and let K^j be the union of the first j lower stars, $K^j = \bigcup_{1 \leq i \leq j} \underline{\mathrm{St}}\, u^i$. The subcomplex K^j of K consists of the j lowest vertices together with all edges and triangles connecting them. We call $K^1, K^2, \ldots, K^n$ a *filtration* of K. Let β_0^j, β_1^j, and β_2^j be the three possibly non-trivial Betti numbers of K^j. For example $\beta_0 = \beta_0^n = 1$, $\beta_1 = \beta_1^n$, and $\beta_2 = \beta_2^n = 1$ are the Betti numbers of $K = K^n$. The Betti numbers of K^{j+1} can be computed from those of K^j merely by looking at the type of u^{j+1} and how its lower star connects to K^j [6]. It is convenient to adopt reduced homology groups, but we will freely talk about components and holes when we mean reduced homology classes of non-bounding 0- and 1-cycles. We start with $\beta_{-1}^0 = 1$ and $\beta_0^0 = \beta_1^0 = \beta_2^0 = 0$. Regular vertices u^{j+1} can be skipped because they do not change the Betti numbers.

Case 0 (u^{j+1} is a minimum). If $j + 1 = 1$ then $\beta_{-1}^1 = \beta_{-1}^0 - 1 = 0$. Otherwise u^{j+1} forms a new component and we increment the zero-th Betti number to $\beta_0^{j+1} = \beta_0^j + 1$.

Case 1 (u^{j+1} is a k-fold saddle). The lower star touches K^j along $k + 1$ simple paths. Let $1 \leq \gamma \leq k + 1$ be the number of touched components. Then, the lower star decreases the number of components to $\beta_0^{j+1} = \beta_0^j - (\gamma - 1)$ and increases the number of holes to $\beta_1^{j+1} = \beta_1^j + (k + 1 - \gamma)$.

Case 2 (u^{j+1} is a maximum). If $j + 1 = n$, then adding the lower star completes the manifold and $\beta_2^n = \beta_2^{n-1} + 1 = 1$. Otherwise, the lower star closes a hole and we decrement the first Betti number to $\beta_1^{j+1} = \beta_1^j - 1$.

The Betti numbers change as components and holes are created and destroyed. Every minimum, except the first, creates a non-bounding 0-cycle. Every maximum, except the last, destroys a non-bounding 1-cycle. Every simple saddle either destroys a component, if $\gamma = 2$, or creates a hole, if $\gamma = 1$. A k-fold saddle has the accumulated effect of the k simple saddles.

Persistence. The idea of persistence is the realization that acts of creation can be paired with acts of destruction. Call a critical point *positive* if it creates and *negative* if it destroys. Assume that all saddles are simple, or equivalently, that all multiple saddles have been unfolded. We pair every negative saddle with a preceding positive minimum and every negative maximum with a preceding positive saddle.

To determine the pairs, we scan the filtration from left to right. A positive minimum starts and represents a new component. A negative saddle connects two components of the complex it is added to. Each component is represented by its

lowest minimum, and the saddle is paired with the higher of the minima. The other yet unpaired minimum lives on as the representative of the merged component. A positive saddle starts and represents a new non-bounding cycle. A negative maximum fills a hole in the complex. The boundary of that hole is homologous to a sum of cycles, each represented by a positive saddle. The maximum is paired with the highest of these saddles, and the other saddles live on as representatives of their respective cycles.

At the end of this process, we have minimum-saddle pairs, saddle-maximum pairs, and a collection of $\beta_0 = 1$ minima, β_1 simple saddles, and $\beta_2 = 1$ maxima that remain unpaired. The *persistence* of a critical point a is the absolute height difference $p(a) = |h(b) - h(a)|$, if a is paired with b, and $p(a) = \infty$ if a remains unpaired. We illustrate the pairing and the resulting persistence by drawing the critical points on the (horizontal) height axis as shown in Figure 13.

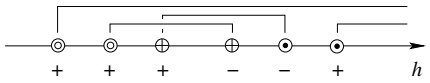

Figure 13: Each critical point is either positive or negative. The persistence is the absolute height difference between paired critical points.

We may also assemble a triangulation in the order of decreasing height. Define L^{n-j+1} as the union of the upper stars of the j highest vertices. The sequence $L^n, L^{n-1}, \ldots, L^1$ is again a filtration of K, and we can compute Betti numbers as before. Because of the reversal of direction, minima and maxima exchange their roles in the Betti number algorithm, and negative critical points act like positive ones and vice versa. Although everything is reversed, the persistence of critical points remains unchanged. In other words, we have the same pairing of critical points, regardless of the direction of assembly for the filtration.

Computation. We compute the pairing of critical points and their persistence using the algorithm given in [7]. Instead of applying that algorithm to a sequence of critical points (as described above), we apply it to a sequence of simplices. In the ascending direction, the appropriate sequence is obtained by replacing each critical point u^i by the simplices in its lower star, ordered by non-decreasing dimension. The persistence algorithm pairs most simplices in a lower star with other simplices in that set. The number and dimensions of the simplices that are not paired within the lower star are characteristic for the type of the critical point u^i. Specifically, there is one unpaired vertex if u^i is a minimum, there are k unpaired edges if u^i is a k-fold saddle, and there is one unpaired triangle if u^i is a maximum. We use this characterization to find and classify critical points in practice.

The algorithm that pairs critical points is similar to but different from the constructive definition given above. The minimum-saddle pairs are found by scanning the filtration from left to right. For each negative saddle we determine the matching positive minimum by searching backwards. With the help of a union-find data structure storing the components, this can be done in time $O(nA^{-1}(n))$, where $A^{-1}(n)$ is the notoriously slow growing inverse of the Ackermann function. Symmetrically, the saddle-maximum pairs are found by scanning the reversed sequence of simplices that corresponds to the filtration of the L^j. The running time is again $O(nA^{-1}(n))$. Note that the two-scan algorithm makes essential use of the fact that persistence is symmetric with respect to increasing and decreasing height. We could also find the saddle-maximum pairs in the first scan, but the running time would be worse as the search for the matching saddle in that direction cannot be accelerated by using a union-find data structure.

7 Hierarchy

Given a Morse complex, we create a hierarchy by successive simplification. Each step in the process cancels a pair of critical points and the sequence of cancellations is determined by the persistence of the pairs.

Cancellation. To simplify the discussion consider first a generic one-dimensional height function $f : \mathbb{R} \to \mathbb{R}$. Its critical points are minima and maxima in an alternating sequence from left to right. In order to eliminate a maximum we locally modify f so that the maximum moves towards an adjacent minimum. When the two points meet, they momentarily form a degenerate critical point and then disappear, as illustrated in Figure 14. Clearly, only adjacent critical points

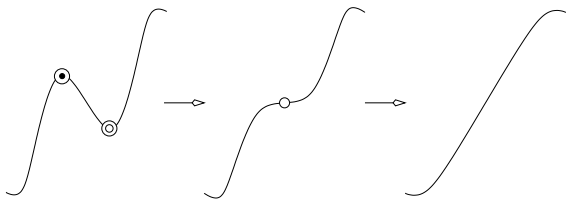

Figure 14: The cancellation of a minimum-maximum pair.

can be cancelled, but adjacency is not sufficient unless we are willing to modify f globally. We also require that the height difference between the two critical points is less than that of pairs in the neighborhood. In Figure 15, the pairs computed by the persistence algorithm and plotted along the domain axis are either disjoint or nested. We cancel pairs of critical points in the order of increasing persistence. The nesting structure is thus unraveled from inside out by removing one innermost pair after the other.

Simplification. We now return to our height function h over $\mathbb{M}$. The critical points of h can be eliminated in a very similar manner by locally modifying the height function. In

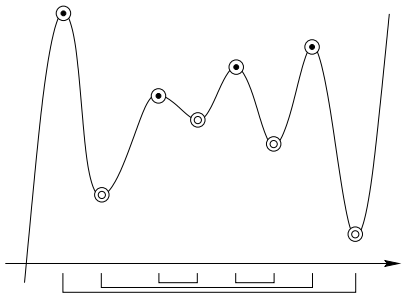

Figure 15: The intervals defined by critical point pairs are either disjoint or nested.

the generic case, the critical points cancel in pairs of contiguous indices. More precisely, positive minima cancel with negative saddles and positive saddles cancel with negative maxima. We simulate the cancellation process combinatorially by removing critical points in pairs from the Morse complex. Figure 16 illustrates the operation for a minimum b paired with a saddle a. The operation requires that ab be an arc in the complex. Let c be the other minimum and d, e the two maxima connected to a. We delete the two ascending paths from a to d and e, and contract the two descending paths from a to b and c. In the symmetric case in which b is a maximum, we delete the descending and contract the ascending paths. The contraction pulls a and b into the critical point c, which inherits the connections of b. We call this operation the *cancellation* of a and b. It is the only operation needed in the construction of the hierarchy. There are two special cases, namely when $d = e$ and when $b = c$, which cannot occur at the same time. In the latter case, we prohibit the cancellation as it would change the topology of the 2-manifold.

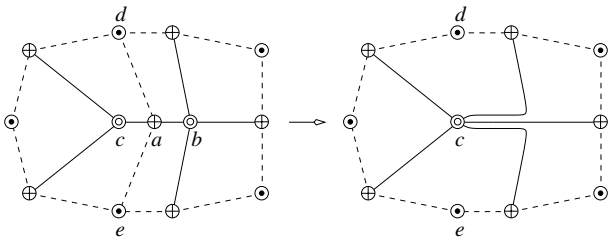

Figure 16: The cancellation of a and b deletes the arcs ad and ae and contracts the arcs ca and ab. The contraction effectively extends the remaining arcs of b to c.

The sequence of cancellations is again in the order of increasing persistence. In general, not every two critical points paired by the persistence algorithm are adjacent in the Morse complex. We prove that they will be adjacent at the required time, even if the initial quasi Morse complex Q is a poor approximation of the Morse complex.

ADJACENCY LEMMA. For every positive i, the i-th pair of critical points ordered by persistence forms an arc in the complex obtained by cancelling the first $i-1$ pairs.

PROOF. Assume without loss of generality that the i-th pair consists of a negative saddle $a = u^{j+1}$ and a positive minimum z. Consider the component of K^j that contains z. One of the descending paths originating at a enters this component and because it cannot ascend it eventually ends at some minimum b in the same component. Either $b = z$, in which case we are done, or b has already been paired with a saddle $c \neq a$. In the latter case, c has height less than a, it belongs to the same component of K^j as b and z, and b, c is one of the first $i - 1$ pairs of critical points. It follows that when b gets cancelled, the path from a to b gets extended to another minimum d, which again belongs to the same component. Eventually, all minima in the component other than z are cancelled, implying that the initial path from a to b gets extended all the way to z. The claim follows. □

8 Results for Terrains

This section presents experimental results to support the viability of our approach for analyzing geographic terrain data. At the time of submission, we have only implemented the algorithms for constructing quasi Morse complexes and the persistence of critical points. We shall add experimental results for the remaining algorithms as they become available.

Data sets. We use three rectangle sections of rectilinear grid elevation data of Earth [12] and one synthetic data sampled from $h(x, y) = \sin x + \sin y$ for input. The names and sizes of the data sets are given in Table 1. In each case, we convert the gridded rectangle into a triangulated sphere by adding diagonals to the square cells and connecting the boundary edges and vertices to a dummy vertex at height minus infinity. We show the quasi Morse complex of data set Sine in Figure 17. It is computed by the algorithm presented in Section 4, and it is also the Morse complex, in this case. In Figure 18, we display the terrain of Iran along with its quasi Morse complex.

	grid size	# simplices
Sine	100×100	59,996
Iran	277×229	380,594
Himalayas	469×265	745,706
Andes	385×877	2,025,866
North America	793×505	2,402,786

Table 1: The four data sets. The second column counts all vertices, edges, and triangles of the triangulations.

Statistics. We first compute a filtration of the sphere triangulation by sorting the simplices in the order of increasing

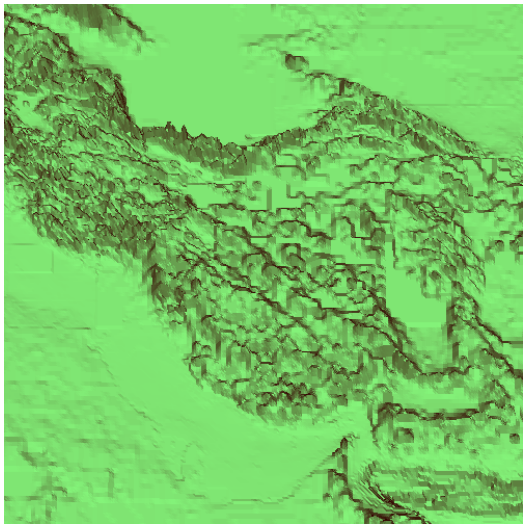

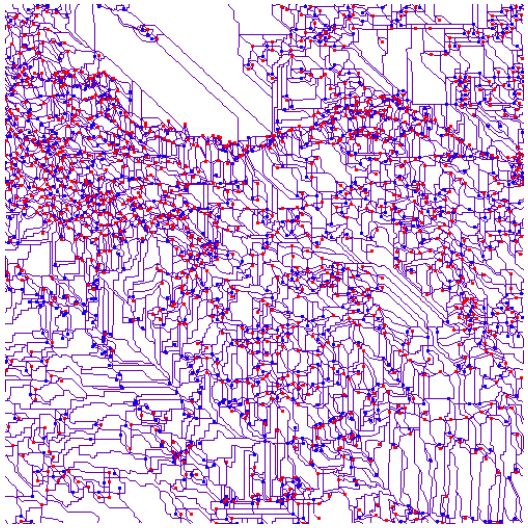

Figure 18: Iran's Alburz mountain range borders the Caspian sea (top flat area), and its Zagros mountain range shapes the Persian Gulf (left bottom.) We show a rendering of the terrain and its quasi Morse complex.

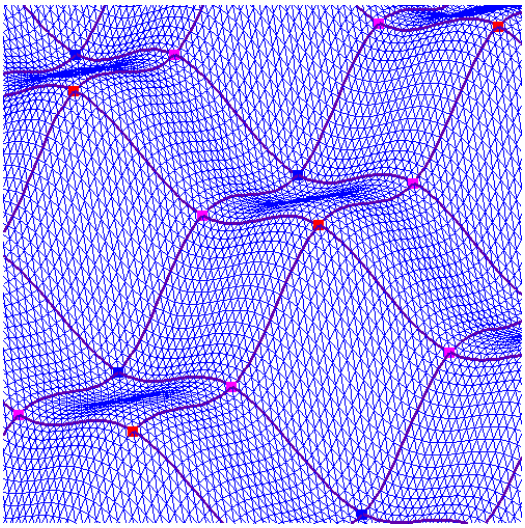

Figure 17: The Morse complex partitions triangulated sampled data from $h(x, y) = \sin x + \sin y$.

height, as explained in Section 6. We then use the persistence algorithm to compute and classify the critical points. Table 2 shows the number of critical points of each type. Since we start with grid data and add diagonals in a consistent manner, each vertex other than the dummy vertex has degree at most six. We can therefore have monkey saddles in our data but no saddles of multiplicity higher than two. The current implementation constructs only one filtration and computes persistence in a single scan, forfeiting the benefit of a union-find data structure for pairing maxima with saddles. Table 3 shows the running time of constructing the filtration,

	# Min	# Sad	# Mon	# Max
Sine	10	24	0	16
Iran	1,302	2,786	27	1,540
Himalayas	2,132	4,452	51	2,424
Andes	20,855	38,326	1,820	21,113
North America	15,032	30,733	464	16,631

Table 2: The number of critical points of the four triangulated spheres. Note that $\#\text{Min} - \#\text{Sad} - 2\#\text{Mon} + \#\text{Max} = 2$ in each case, as it should be.

computing the persistence information, and constructing the quasi Morse complex.

	filt	pers	qM
Sine	0.06	0.13	0.03
Iran	0.46	0.90	0.56
Himalayas	0.89	1.74	1.01
Andes	2.62	4.90	2.60
North America	3.28	5.84	5.26

Table 3: Running times in seconds. All timings were done on a Sun Ultra-10 with a 440 MHz UltraSPARC IIi processor and 256 megabyte RAM, running the Solaris 8 operating system.

9 Conclusion

This paper introduces Simulation of Differentiability as a computational paradigm, and uses it to construct Morse complexes of PL height functions over compact 2-manifolds without boundary. It also uses topological persistence to build a

hierarchy of progressively coarser Morse complexes.

Our results complement and improve related work in visualization [1, 5, 13] and computational geometry [3, 4, 14], but many questions remain. Can we go from a quasi Morse to the Morse complex by performing handle slides in an arbitrary sequence, as opposed to ordering them by height? How can we take advantage of the Morse complex structure and cancel critical points in a controlled manner through smoothing or locally averaging the height function? What are the dependencies between different critical points, and how does a cancellation interfere with non-participating critical points?

There are at least three interesting challenges in generalizing the results of this paper. Can we use hierarchical methods similar to the ones in this paper to simplify medial axes of two-dimensional figures? Can we extend our methods to more general vector fields? Can we extend our results to height functions over 3-manifolds? The generalization of the Morse index of critical points to the Conley index of isolated neighborhoods [11] might be useful in answering the second question.

References

[1] BAJAJ, C. L., PASCUCCI, V., AND SCHIKORE, D. R. Visualization of scalar topology for structural enhancement. In *Proc. 9th Ann. IEEE Conf. Visualization* (1998), pp. 18–23.

[2] BANCHOFF, T. F. Critical points and curvature for embedded polyhedral surfaces. *Am. Math. Monthly* **77** (1970), 475–485.

[3] CARR, H., SNOEYINK, J., AND AXEN, U. Computing contour trees in all dimensions. In *Proc. 11th Ann. Sympos. Discrete Alg.* (2000), pp. 918–926.

[4] DE BERG, M., AND VAN KREVELD, M. Trekking in the alps without freezing and getting tired. In *Proc. 1st Europ. Sympos. Alg* (1993), pp. 121–132.

[5] DE LEEUW, W., AND VAN LIERE, R. Collapsing flow topology using area metrics. In *Proc. 10th Ann. IEEE Conf. Visualization* (1999), pp. 349–354.

[6] DELFINADO, C. J. A., AND EDELSBRUNNER, H. An incremental algorithm for Betti numbers of simplicial complexes on the 3-sphere. *Comput. Aided Geom. Design* **12** (1995), 771–784.

[7] EDELSBRUNNER, H., LETSCHER, D., AND ZOMORODIAN, A. Topological persistence and simplification. In *Proc. 41st Ann. IEEE Sympos. Found Comput. Sci.* (2000), pp. 454–463.

[8] EDELSBRUNNER, H., AND MÜCKE, E. P. Simulation of Simplicity: a technique to cope with degenerate cases in geometric algorithms. *ACM Trans. Graphics* **9** (1990), 66–104.

[9] GUIBAS, L., AND STOLFI, J. Primitives for the manipulation of general subdivisions and the computation of Voronoi diagrams. *ACM Trans. Graph.* **4** (1985), 74–123.

[10] MILNOR, J. *Morse Theory*. Princeton Univ. Press, New Jersey, 1963.

[11] MISCHAIKOW, K., AND MROZEK, M. Conley index theory. In *Handbook of Dynamical Systems III: Towards Applications*, B. Fiedler, G. Iooss, and N. Kopell, Eds. Elsevier, to appear.

[12] NOAA. Announcement 88-mgg-02, digital relief of the surface of the earth, 1988. http://www.ngdc.noaa.gov/mgg/-global/seltopo.html.

[13] TRICOCHE, X., SCHEUERMANN, G., AND HAGEN, H. A topology simplification method for 2D vector fields. In *Proc. 11th Ann. IEEE Conf. Visualization* (2000), pp. 359–366.

[14] VAN KREVELD, M., VAN OOSTRUM, R., BAJAJ, C., PASCUCCI, V., AND SCHIKORE, D. Contour trees and small seed sets for iso-surface traversal. In *Proc. 13th Ann. Sympos. Comput. Geom.* (1997), pp. 212–220.

[15] WALLACE, A. *Differential Topology. First Steps.* W. A. Benjamin, New York, 1968.